Low-Temperature Cr[53] NMR in a Ferromagnetic CrBr₃ Single Crystal

C. H. Cobb[*†]

Southern College of Optometry, Memphis, Tennessee 38104

and

V. Jaccarino[*]

Department of Physics, University of California, Santa Barbara, California 93106

and

M. A. Butler and J. P. Remeika

Bell Laboratories, Murray Hill, New Jersey 07974

and

H. Yasuoka[*†]

Department of Metal Science and Technology, Kyoto University, Kyoto, Japan

The properties of the Cr[53] NMR in a single crystal of ferromagnetic CrBr₃ were studied at low temperatures. From the dependence of the observed resonances on the orientation of the magnetic field with respect to the easy axis of magnetization and the magnitude of the enhancements of the driving rf field it is shown that all of observed spectra must arise from nuclei belonging to spins that, in the main, are at the center and edge of 180° walls, in the unsaturated state. Using a model which incorporates a position-dependent linewidth within the wall a reasonable simulation of the observed spectra is made. The predicted dependence of the domain rotation enhancement, above saturation, on the magnitude and orientation of the external field is observed. Some implications of these results for other NMR studies in ferromagnets are discussed.

I. INTRODUCTION

The study of the magnetic properties of CrBr₃, one of the few ferromagnetic insulators,[1] has made possible a detailed comparison of experiment with the predictions of spin-wave theory for a Heisenberg ferromagnet.[2-4] Until recently, nuclear-magnetic-resonance (NMR) measurements have been confined to powders and, therefore, to the case of no external magnetic field.

In the present work a series of NMR studies on a CrBr₃ single crystal provide a further understanding of the magnetic properties of a ferromagnetic insulator. In the first paper[5] we gave the results of an experimental and theoretical investigation of the field and temperature dependence of the magnetization $M(T, H)$ as deduced from the Cr[53] NMR frequency dependence. The present paper considers in detail the character of the observed resonances, with particular emphasis on their origin and nature of excitation.

Section II details the equipment and measurement techniques for the various experiments, while Sec. III presents the results. Measurements have been made of the dependence of the Cr[53] NMR frequencies and signal intensities on the magnitude and direction of the external dc field and the signal-intensity dependence on rf polarization. The rf-field enhancement has been measured using fast-passage and rotary-saturation techniques. In Sec. IV these results are used to identify the orientation and character of the spins contributing to the resonances. Particular attention is paid to the nature of the enhancement mechanisms and the implication these results have for resonance measurements in other ferromagnetic materials.

II. EXPERIMENTAL DETAILS

The CrBr₃ sample used in these experiments is a single crystal measuring approximately $5 \times 11 \times 16$ mm³, with the uniaxial c axis oriented perpendicular to the largest side. Details of the procedure for growing a single crystal were described in a previous paper.[5] Although it would be desirable to study a sample that is ellipsoidal in shape to eliminate inhomogeneous broadening of the resonance lines when the sample is saturated, the tendency of CrBr₃ to flake and deform[6] when cut prevented us from doing this. Assuming the crystal to have an approximately ellipsoidal shape, we estimate the appropriate demagnetizing factors to be $N_D^{\parallel} \simeq 0.8(4\pi)$ and $N_D^{\perp} \simeq 0.1(4\pi)$ for the external field parallel and perpendicular to the c axis, respectively. Since the saturation magnetization of CrBr₃ at $T = 0$ °K is $M_S = 0.27$ kOe,[1] we would expect technical saturation to occur at fields of $H_s^{\parallel} = N_D^{\parallel} M_s = 2.7$ kOe and $H_s^{\perp} = H_A + N_D^{\perp} M_s = 7.1$ kOe. We shall see that the NMR studies provide an accurate measurement of $H_s^{\parallel}$ and $H_s^{\perp}$ which agrees with the above estimates.
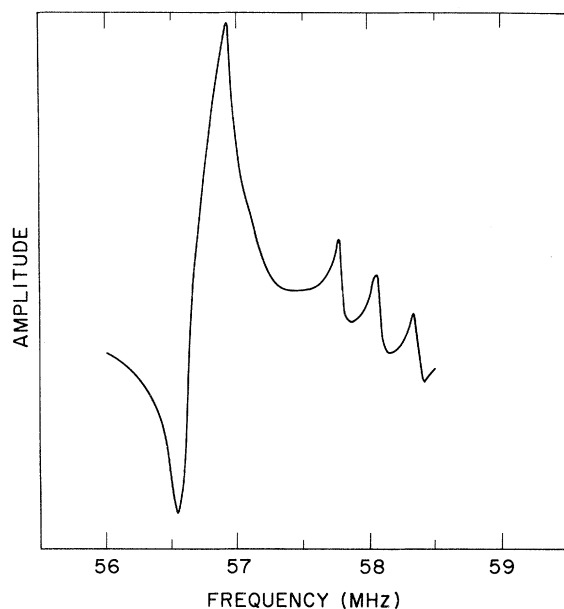
FIG. 1. Recorder trace of the derivative of the ob-
served Cr^{53} NMR spectrum in $CrBr_3$ at 1.4 °K. The three
quadrupolar components of the a resonance appear on the
right-hand side of the spectrum and the strong b reso-
nance is seen on the left-hand side.

The sample was mounted in a helium cryostat
so that any orientation of the dc magnetic field H_0
with respect to the c axis could be obtained. To
inhibit the decomposition of the crystal through
hydration, exposure of the sample to air was
minimized. Desired temperatures in the liquid-
helium and -hydrogen ranges were achieved by
suitably adjusting the vapor pressure above the
liquid. Accurate calibration of the dc field was
obtained from proton NMR frequency measurements.

Whenever it was possible, measurements were
made with a push-pull marginal oscillator[7] opera-
ted in the 40–60-MHz region at an rf level corre-
sponding to an $H_{rf} \simeq 0.01$ Oe at the sample. Unfor-
tunately, the oscillator had to be kept in the fring-
ing field of the dc magnet and the sensitivity of the
resonance system decreased with increasing H_0.
The sensitivity could be increased by operating in
a superregenerative mode, with the strength of the
rf field increased to a maximum of $H_{rf} \simeq 0.1$ Oe.
However, the superregenerative oscillator dis-
played a similar field dependence to its sensitivity
as the marginal oscillator. Nevertheless, in this
manner all resonances could be studied for fields
below saturation, with $\vec{H}_0 \parallel \vec{c}$ axis. In the region
where the resonances could be detected by both
marginal and superregenerative methods, identical
results were obtained.

With the external field oriented perpendicular to
the easy c axis, saturation occurs at a field $H_0^\perp$

almost twice as large as the maximum field for
which a steady-state signal could be observed.
Because of this difficulty, transient techniques were
also employed. The large pulsed rf fields (H_{rf}
~ 1–10 Oe) made for increased sensitivity and,
since the pulsed oscillator was well removed from
the dc field, it was not disturbed by changes in the
external field. The increased sensitivity was par-
ticularly useful for $H_0 > H_s$, since the enhancement
of the NMR signal decreases markedly once satu-
ration is achieved. For those fields where both
steady-state and transient signals could be observed,
identical results were obtained for the frequency
for resonance to within experimental error. For
the transient studies[8] pulses were applied to a LC
resonance circuit and the detected signal passed
through a broad-band amplifier before presentation
on an oscilloscope. The Q of the resonant circuit
restricted spin-echo observations to times $2\tau \geq 18$
μsec.

In order to measure the rf-field enhancement
using the technique of rotary saturation,[9] two sep-
arate ac frequency-modulation signals were applied
to a varactor in the marginal-oscillator resonance
circuit. One signal provides the alternating field
for rotary saturation and the other the field for
detection; the one used for phase-sensitive detec-
tion was 100 Hz, while the rotary-saturation fre-
quency could be varied from 0 to a maximum of
80 kHz. For frequencies above 80 kHz, the oscil-
lator quenched and behaved as a superregenerative
oscillator. To test the effectiveness of our pro-
cedures, the rotary saturation of Fe^{57} in Fe metal
was studied with results identical to those obtained
by Mendis and Anderson,[10] to within experimental
error.

III. EXPERIMENTAL OBSERVATIONS

A. Resonance Frequencies

In zero external field what appear to be two
distinct Cr^{53} resonances have been observed,[5] as
shown in Fig. 1, where the derivative of the spec-
trum is displayed. These resonances will be des-
ignated the type-a resonance and the type-b reso-
nance throughout this paper. At the lowest tem-
perature (~ 1.4 °K) the resonances have the follow-
ing properties.

$H_0 = 0$. The a resonance consists of three quad-
rupole-split resonances centered at 58.056 MHz.
Each of the component resonances has an apparent
half-width at half-intensity of 16 kHz. Of the three
components the satellite resonances are weaker
than the central one by about 30%. All of the a
resonances could be observed by both steady-state
and transient NMR techniques. The a resonances
have been studied previously[2] in a polycrystalline
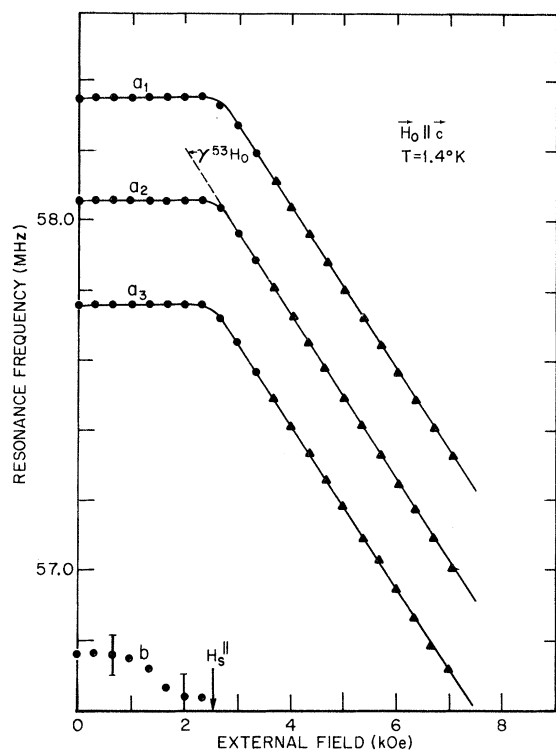sample, and our results agree with the polycrys-

FIG. 2. Cr^{53} NMR a and b resonance frequencies as a function of field H_0, with H_0 applied parallel to the c axis. The field at which the sample saturates $H_s^{\parallel}$ is indicated by the vertical arrow in the lower part of the figure. The dashed line marked $\gamma^{53} H_0$ is the slope of the ν-vs-H line calculated from the known γ^{53}, assuming the hyperfine and external fields to be oppositely directed.

tal work except that, in the latter case, the widths are almost double the single-crystal ones.

The b resonance appears to be a single, broad, intense resonance centered at 56.766 MHz at 1.4 °K. It has an apparent half-width at half-intensity of 360 kHz and a more complex line shape than the a resonances. Of particular interest is that it could only be observed by steady-state NMR techniques. The b resonance has also previously been observed[3] in a polycrystalline sample where the results, as well as similar measurements we have made on a polycrystalline sample, agree with the above except that the polycrystal linewidth again is larger by a factor of 2.

$\vec{H}_0 \parallel \vec{c}$. The external magnetic field dependence of the Cr^{53} NMR frequency for both a and b resonances is shown for H_0 applied parallel to the c axis in Fig. 2. For the three a resonances, the NMR frequencies, as well as the spacing between them, were observed to be independent of field for $H_0 < H_0^{\parallel} = 2.5$ kOe. The apparent widths of each of these resonances increase from 16 to 19 kHz as H_0 is raised from 0 to 2 kOe. With increasing field the b resonance appeared to become more complex

in shape and to increase in apparent width from 360 kHz in zero field to 452 kHz at 2 kOe.

For $H_0 > H_s^{\parallel}$, only three narrow resonances are observed, which appear to be the continuation of the a resonances. Their field dependence is given by $\gamma_n H_0$ to within experimental error, where γ_n is the nuclear gyromagnetic ratio for Cr^{53} (see Fig. 2). Because the data given in Fig. 2 are for $T = 0.04 T_c$ (1.4 °K), at which point $M(T)$ is very close to $M(0)$, the change in γ_n which results from the induced paramagnetic frequency shift is insignificant. The spacing between the three resonances remains field independent in the saturated region. Accurate line-shape and linewidth measurements could not be made for $H_0 > H_s^{\parallel}$ using the pulse-detection methods (see Sec. II).

$\vec{H}_0 \perp \vec{c}$. For the external magnetic field applied perpendicular to the c axis, the field dependence of the Cr^{53} NMR frequencies is shown in Fig. 3. The frequencies of the three a resonances, as well as the spacing between them, were observed
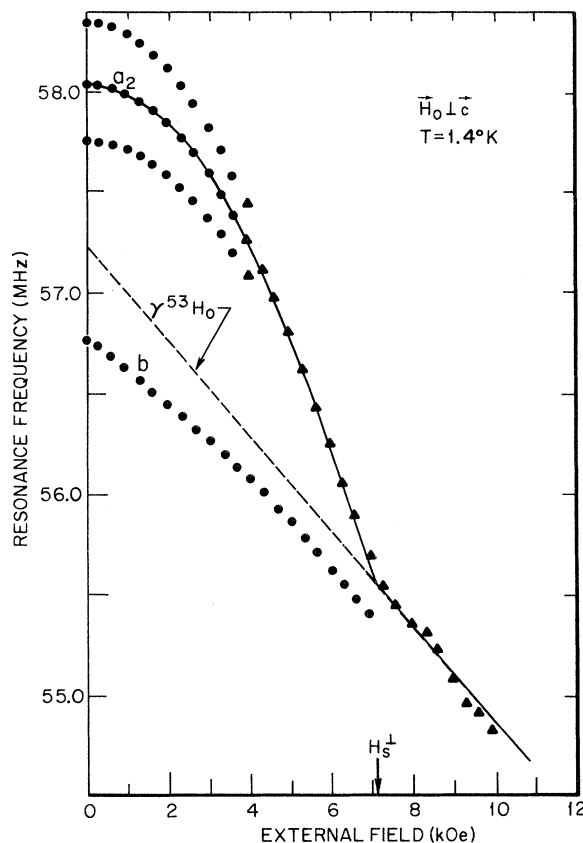

FIG. 3. Cr^{53} NMR a and b resonance frequencies as a function of field H_0, with H_0 applied perpendicular to the c axis. The field at which the sample saturates $H_s^{\perp}$ is indicated by the vertical arrow in the lower part of the figure. The dashed line is explained in the caption to Fig. 2.
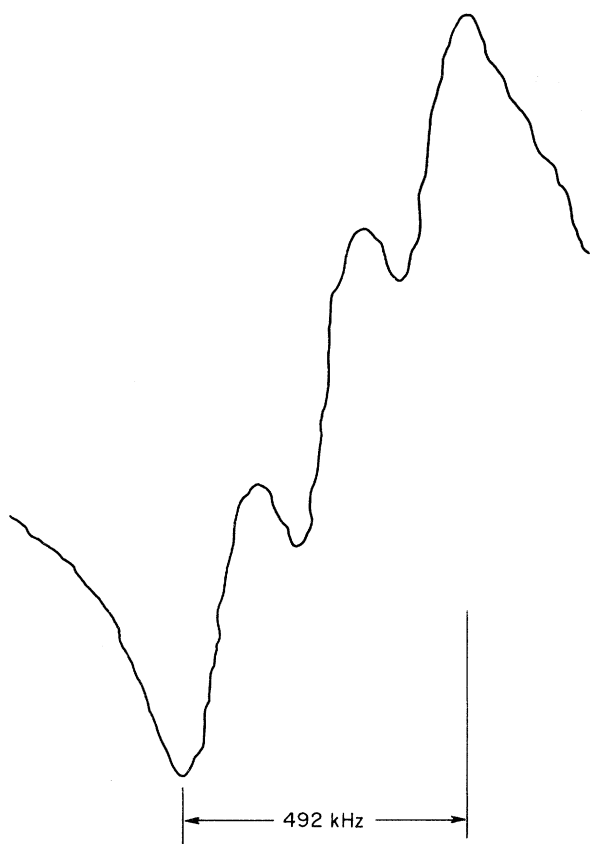
FIG. 4. Derivative of the Cr^{53} b resonance vs frequency in a perpendicularly oriented field; $H_0^\perp \simeq 6$ kOe. The spacing between the quadrupolar components is exactly half that which is observed for the a resonance for all values of $H_0^\parallel$ and equal to the observed spacing for $H_0^\perp > H_s^\perp$. The frequency increases from left to right but in a slightly nonlinear fashion.

to decrease nonlinearly with increasing fields when $H_0 < H_s^\perp = 7.1$ kOe. At $H_0 = H_s^\perp$, the spacings between the three a resonances are exactly half of their zero-field value. The line shape and apparent width of each of the a resonances are similar to those observed for $\vec{H}_0 \parallel \vec{c}$, with the measurements again confined to $0 < H_0 < 2$ kOe because of the field sensitivity of the cw oscillator. The b resonance frequency also initially decreased nonlinearly with increasing fields when $H_0 < H_s^\perp$, but the decrease was not as fast as for the a resonances and approached a straight line with slope γ_n as H_0 approached $H_s^\perp$. A cw signal could be detected for the more intense b resonance for all fields less than $H_s^\perp$. The b line profile develops a structure as the field increases, revealing the presence of three lines. These three b lines become well resolved at $H_0 = 6$ kOe, as shown in Fig. 4, with a field-independent spacing exactly one-half of that which the three a resonances have in zero field.

The apparent half-width at half-intensity of each of the resonances is approximately 90 kHz at 6 kOe.

For $H_0 > H_s^\perp$, only a transient signal could be observed, corresponding to three relatively narrow lines whose field-independent spacings were one-half the a resonance spacings in zero field. Again, the field dependence of the resonance frequency was $\gamma_n H_0$, to within the experimental error.

In the field range 0–2 kOe the transient NMR signal for each of the a resonances is dominated by a free-induction decay which is modulated by the electric quadrupole interaction.[11] No spin-echo signal is observed at these fields, presumably because it is hidden beneath the free-induction decay. However, as H_0 is raised, the free-induction signal begins to decay more rapidly and from $2 < H_0 \lesssim 10$ kOe a spin-echo signal may be detected, the upper bound being determined by signal-to-noise considerations. For the a resonance the echo-determined T_2 was observed to be independent of field, above 2 kOe, with $T_2^a = 55$ μsec for $\vec{H}_0 \perp \vec{c}$ and $T_2^a = 75$ μsec for $\vec{H}_0 \parallel \vec{c}$. Both the free-induction decay and the spin-echo signals were observed for the a resonances over a large range of rf fields. However, neither could be observed for the b resonances *for any field or at any temperature*, from which we infer that T_2^b always remains less than 9 μsec.

In zero applied field, the ratio of integrated intensities of the three unresolved b resonances to the central a resonance is approximately 20. (This result, surprisingly, is independent of the orientation of the transverse rf field with respect to the crystal axes.)

B. Enhancement

Since the angle θ through which a spin turns when subjected to a transverse rf-field pulse H_1 of duration τ_p is

$$\theta = \gamma_n H_1 \tau_p , \tag{1}$$

one could obtain the enhancement $\eta = H_1/H_{rf}$ directly from a measurement of θ. This is difficult to accomplish directly. However, the spin-echo amplitude is a function of θ. For a single resonance broadened by magnetic field inhomogeneities a $\frac{1}{2}\pi$-π pulse sequence yields the largest spin-echo amplitude. The optimum pulse sequence when a quadrupole interaction is present depends on the nature of the nuclear spin-spin interaction and may be further complicated by field inhomogeneities.[12] Being somewhat uncertain as to the latter effects we have undertaken only *relative* measurements of the optimum H_{rf} required to maximize the echo amplitude for $H_0 > H_s$. (For $H_0 < H_s$ η is so large that no combination of H_{rf} and τ_p available with our equipment allowed for maximizing the echo signal). The results of the en-
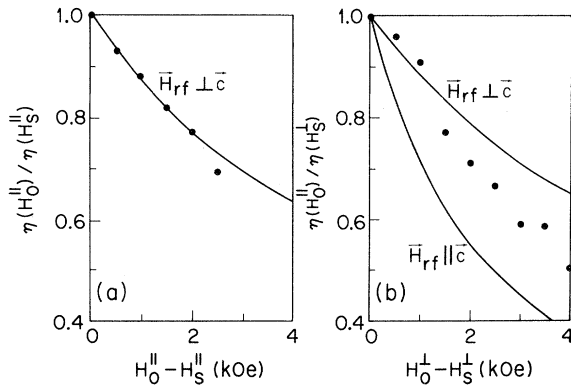
FIG. 5. Enhancements of the Cr^{53} NMR in $CrBr_3$, for (a) $H_0^{\parallel} > H_s^{\parallel}$ and (b) $H_0^{\perp} > H_s^{\perp}$ measured relative to the value at saturation, in the respective directions. The polarizations of the rf field in each case are indicated on the theoretical curves [Eqs. (4a)–(4c)]. Due to sample and coil geometries we believe the data shown in (b) are an unknown mixture of the two polarizations.

hancement measurements for $H_0 > H_s^{\parallel}$ and $H_0 > H_s^{\perp}$ are shown in Figs. 5(a) and 5(b), respectively.

Obviously, it is desirable to have detailed knowledge of η for $H_0 < H_s$—particularly so in view of the difference in intensities between the a and b resonances and the apparent absence of appreciable rf polarization effects, as might be expected for wall- and domain-motion-enhancement mechanisms. Fortunately, there are two steady-state NMR techniques available to measure η—the fast-passage and rotary-saturation methods.

The fast-passage method utilizes two facts: (i) The NMR signal in a ferromagnet is a mixture of absorption and dispersion and the absorptive component saturates at a lower rf field than does the dispersive one; (ii) the ratio of the dispersive component (i.e., the one 90° out of phase with the modulation) to the in-phase component is[13]

$$\frac{\chi_{90}'}{\chi_0'} \approx \frac{\Delta\omega}{\gamma_n \eta H_{rf}}, \tag{2}$$

provided that $\omega_m^2 T_1 T_2 \gg 1$. Here $\Delta\omega$ is the resonance linewidth and ω_m the modulation frequency.

TABLE I. Enhancement factors for the a and b resonances for different polarizations of the rf field with respect to the c axis. Only the fast-passage method could be used for measuring η_b.

Orientation of $\vec{H}_{rf}$	Rotary saturation $\eta_a \times 10^4$	Fast passage $\eta_a \times 10^4$	Fast passage $\eta_b \times 10^4$	Calculated for center of wall $\eta_W \times 10^4$
$\hat{z} \parallel \vec{c}$	16	5	80	55
$\hat{y}$	1	0.4	20	
$\hat{x}$	12	6	110	
Polycrystal	6	3	20	

Independent measurements of χ_{90}'/χ_0', $\Delta\omega$, and H_{rf} suffice to determine η. The values of the enhancements η_a and η_b for the a and b resonances, respectively, obtained in this way are listed in Table I.

The rotary-saturation[9] method exploits the fact that at resonance, in the "rotating frame," the nuclear magnetization is quantized along H_{rf}, which is perpendicular to the hyperfine field. Hence a second alternating field of frequency ω_{rot} applied parallel to the hyperfine field will cause a reduction in the detected NMR signal when $\omega_{rot} = \gamma_n H_{rf}\eta$.[10] Measuring the amplitude of the detected signal as a function of the frequency of the second alternating field and independently measuring the amplitude of H_{rf} allows η to be determined. The values η_a so obtained, for different orientations of H_{rf}, are also listed in Table I, and the amplitude of the detected NMR signal at resonance as a function of the frequency of the second alternating field ω_{rot} is shown in Fig. 6. It was not possible to use this method to obtain values for η_b since the rotary-saturation resonance frequency was so high as to cause the marginal oscillator to "quench" at a rate determined by ω_{rot}.

IV. INTERPRETATION OF NMR RESULTS

A. Preliminary Considerations

Ideally, all of the experimental observations should have some unique interpretation in terms of a model that adequately describes both the unmagnetized and saturated states of $CrBr_3$ at low temperatures. However, the gross magnetic properties are less sensitive to the peculiarities of domain wall motion than is the NMR, particularly so because the latter reflects pronounced enhancement effects. We must begin, therefore, with some qualitative considerations that serve to iden-
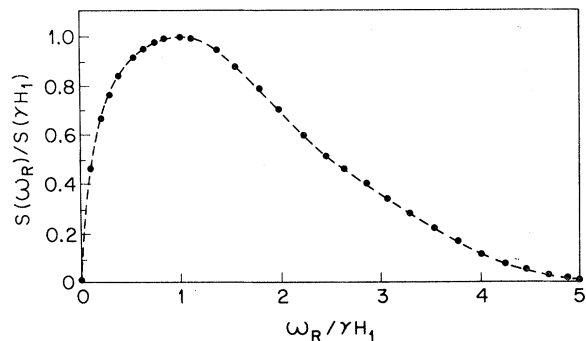

FIG. 6. Plot of the amplitude of the a resonance rotary-saturation signal vs the rotary-saturation frequency. Both are normalized to that value at which the rotary-saturation signal is a maximum. For different values of H_{rf} the $S(\omega_{rot})$-vs-ω_{rot} curves are displaced but, when plotted in the normalized manner shown in the figure, they appear to be identical, within experimental error.

tify the location of the nuclei associated with the a and b resonances, and then see if all of the detailed experimental observations are consistent with the proposed assignments.

We will show that the enhancements measured for both resonances are so large as to preclude their being associated with any process except domain wall motion. From the field dependence of the a and b resonances and their quadrupolar splittings below saturation we will see that the a and b resonance spins are oriented, respectively, *parallel* and *perpendicular* to the spins in the center of the domain. Now the $CrBr_3$ domain structure is known to be a collinear c-axis-oriented one,[1] with 180° walls between the antiparallel domains. *Hence the a resonance must be associated with nuclei of spins at the edge of these walls and the b resonance with those near the center.*

Having made these assertions it behooves us to show that all of the observations are quantitatively consistent with the presumed identification and to show to what extent, if any, they exclude other possible ones. We have to explain (a) the total shielding of the external field at the a and b resonance position when H_0 is applied parallel to the c axis and the apparent penetration of H_0 when it is applied perpendicular to that direction, (b) the frequency variation of both resonances and their quadrupolar splittings as a function of the magnitude and orientation of H_0, and hence the identification of the resonances, (c) the magnitudes of the enhancements and the apparent shapes of the resonances, and finally (d) the rf polarization and rotary-saturation effects.

B. Field Penetration

As regards the matter of the total shielding of the external field, when $\vec{H}_0 \parallel \vec{c}$ and less than $H_s^{\parallel}$, we note that if the primary magnetization process is domain wall motion in an easy-axis ferromagnet then this is precisely what is to be expected; namely, the walls are displaced so as to make the "up" domains larger than the "down" ones, and create a demagnetizing field which just cancels the external field. However, one might regard the apparent exact (to within experimental error) screening of $H_0^{\parallel}$ as rather suspicious, since the non-ellipsoidal shape of the sample should cause a spread in local fields in the sample for values of $H_0^{\parallel} \leq H_s^{\parallel}$. Perhaps this should be regarded as additional evidence for the wall origin of the resonances, since locally the wall will move until the net field acting on the center of the wall vanishes (since otherwise a torque would result and cause further displacement).

When $H_0 > H_s^{\parallel}$, the demagnetizing field can no longer adjust to cancel H_0 and, in the zero-temperature limit, the field dependence of the NMR fre-

quencies would be expected to be $\gamma_n H_0$ (the negative slope above $H_s^{\parallel}$ results from H_{hf} being negative). At finite temperatures this field dependence of the resonance frequency should be modified to include the paramagnetic shift that results from the non-vanishing electronic spin susceptibility. This shift has been both calculated and measured and is discussed in Ref. 5. At the lowest temperature, $T = 1.4$ °K, we expect the shift to be only 3%, which would not be discernible in our experiment.

As to the field penetration perpendicular to the c axis, it should be remarked that the rotation of domain moments, below saturation, results in partial screening of $H_0^{\perp}$, but this happens to be small for our particular sample. The applied $H_0^{\perp}$ is reduced by the factor $H_d^{\perp}(H_s^{\perp})^{-1} \approx 5\%$. This causes the effective γ value of the b nuclear resonance to be smaller by this amount.

We emphasize that in the saturated region *all* of the nuclei in the sample are contributing to the resonance signal, whereas below $H_s^{\parallel}$ it is difficult to identify the number and location of the contributing nuclei, because of the uncertainties associated with the enhancement mechanisms.

C. Identification and Field-Orientation Dependence of Resonances

With $\vec{H}_0 \parallel \vec{c}$, the spacing between the three type-a resonances remains unchanged both above and below $H_s^{\parallel}$. Since for Cr^{53} $I = \frac{3}{2}$, and the gradient of the electric field at the Cr^{3+} position has axial symmetry about the c axis, we conclude that a resonance is to be associated with nuclei whose quantization direction is collinear with the c-oriented domain magnetization and which have a quadrupolar coupling $e^2qQ/2h = 0.297$ MHz. The 3 : 4 : 3 intensity ratio of the three components provides additional confirmation of the quadrupolar character of the a resonance splittings.

Knowing that when $\vec{H}_0 \perp \vec{c}$ the field penetrates the sample and that the a resonance is associated with c-oriented electronic spins we would expect the a resonance frequency to shift as the spins are gradually rotated towards the perpendicular plane. Now the angle θ that the electronic spin moment makes with respect to the c axis at a given value of $H_0^{\perp} \leq H_s^{\perp}$ is specified by the relation $\sin\theta = H_0^{\perp}(H_A + H_d^{\perp})^{-1} = H_0^{\perp}/H_s^{\perp}$. Because $H_{hf} \gg H_0^{\perp}$, the nuclear moments remain essentially aligned along the direction of the electronic magnetization for all values of $H_0^{\perp}$ used in our experiments. Two factors contribute to the behavior of the a resonance frequency with increasing $H_0^{\perp}$: (i) the part of the dipolar field that is anisotropic, and (ii) the large isotropic core-polarization hyperfine field which is negative with respect to the electronic spin moment.

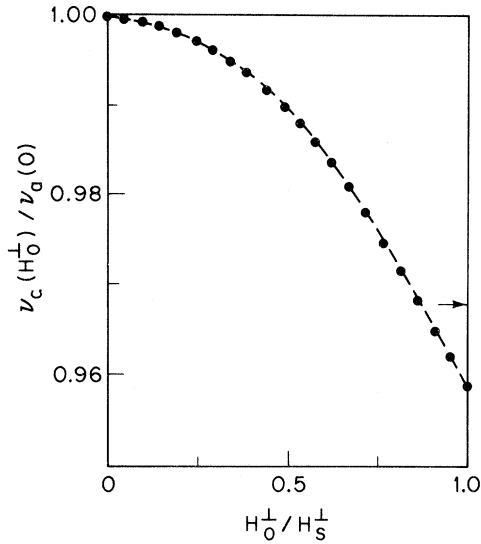The angular dependence of the dipolar-induced

FIG. 7. Observed frequency dependence of the central a resonance as a function of the field applied perpendicular to the c axis. The frequency is normalized to its H $=0$ value and the field to its value at saturation $H_s^\perp$. The quantity $H_0^\perp/H_s^\perp = \sin\theta$ and the dashed line is a calculated curve for the anisotropic contributions to the field at the nucleus assuming they contribute as $\sin^2\theta$. The arrow indicates the dipolar field contribution from just the three nearest-neighbor Cr^{3+} ions at $H_0^\perp = H_s^\perp$.

anisotropy and a rough estimate of its magnitude may be obtained from considering just the three nearest-neighbor Cr^{3+} ions. The anisotropic part of their dipolar field has the form $H_{dip} = (3/2a^3)$ $\times g\mu_B S\sin^2\theta = (3/2\,a^3)\,g\mu_B S\,(H_0^\perp/H_s^\perp)^2$. Again, because $H_{hf} \gg H_0^\perp$, only the projection of the external field along the direction of the spin moment appreciably changes the field at the nucleus. Its contribution has a $H_A(H_0^\perp/H_s^\perp)^2$ dependence, too. The sum of the anisotropic dipolar and external field contributions at $H_0^\perp = H_s^\perp$ measured relative to $H_0^\perp = 0$ is shown by the arrow in Fig. 7. Here we have given the variation in the frequency as a function of $H_0^\perp/H_s^\perp$. If we arbitrarily normalize the anisotropic contributions to agree at $H_0^\perp = H_s^\perp$ we find an almost exact (see dashed line) $H_0^\perp/H_s^\perp$ frequency dependence. Presumably the small difference in the proportionality constant must arise from a combination of more distant moments being neglected and the possibility of an intra-atomic orbital anisotropy being present. It is interesting to note that the observed value of $H_s^\perp = 7.1$ kOe agrees exactly with the calculated value from the known H_A[14] and the rough estimate of the perpendicular demagnetizing factor given in Sec. II. Because of the rough estimate of the demagnetizing, such good agreement must be considered somewhat fortuitous.

The above analysis has been made for the central a resonance, which corresponds to the $\frac{1}{2} \leftrightarrow -\frac{1}{2}$

quadrupole transition. To facilitate the analysis of the satellite a resonances corresponding to the $\pm\frac{3}{2}\leftrightarrow\pm\frac{1}{2}$ quadrupole transitions, we plot in Fig. 8 the difference in frequency between each satellite resonance and the central one as a function of the angle between the c axis and the magnetization. This difference should have an angular dependence to first order[15] given by

$$\Delta\nu(\theta) = \frac{e^2qQ}{4h}\ (3\cos^2\theta - 1)\ . \tag{3}$$

A plot of both Eq. (3) and the experimental difference is given in Fig. 8. In particular we observe $\Delta\nu(\frac{1}{2}\pi)$ $=\frac{1}{2}\Delta\nu(0)$, as predicted by Eq. (3). Above $H_s^\perp$ the NMR frequencies have the proper $\gamma_n H_0$ dependence, with $\Delta\nu$ remaining constant since θ remains fixed at $\frac{1}{2}\pi$.

As regards the b resonances, the best evidence that they are associated with spins which are perpendicular to the c axis comes from the perpendicular field dependence of the resonance and the observed resolution of a quadrupolar splitting at higher fields (6 kOe $\le H_0^\perp < H_s^\perp$); namely, the observed
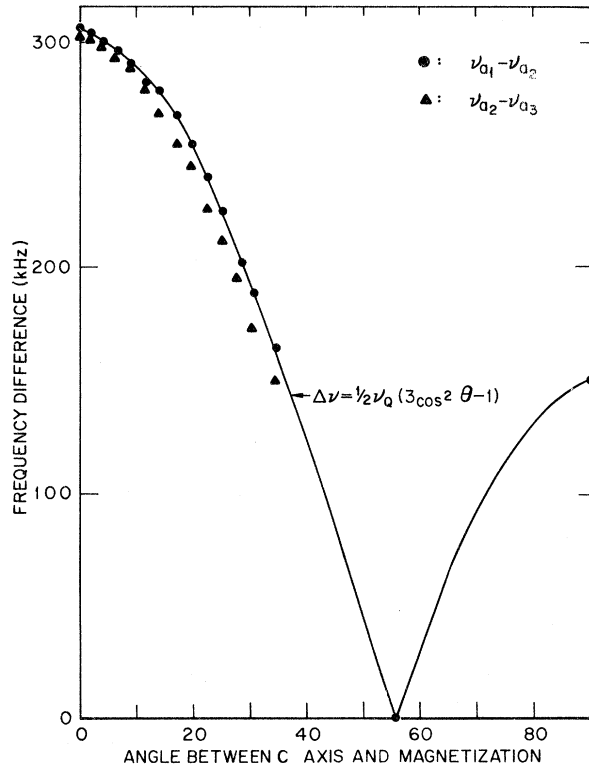

FIG. 8. Observed frequency splittings of the quadrupolar components of the a resonance as a function of the angle between the c axis and the magnetization, when H_0 is applied perpendicular to the c axis. The angle is determined by minimizing the free energy. The expected splitting is shown by the solid curve with ν_Q evaluated at $H = 0$.
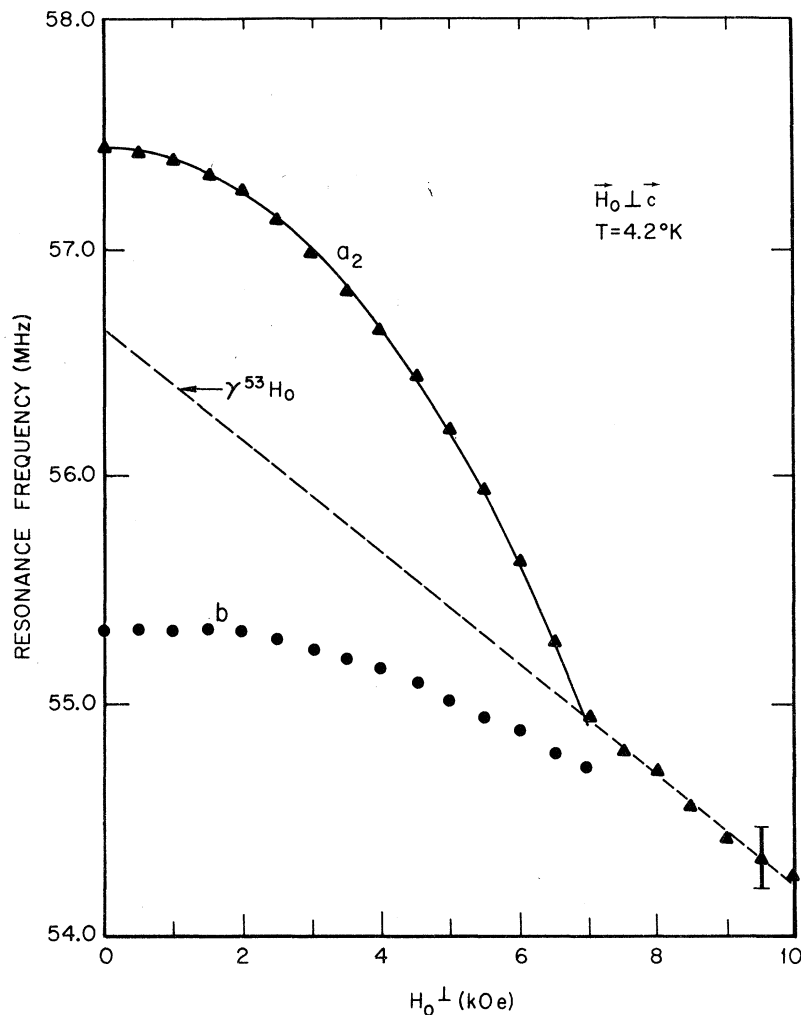
FIG. 9. Frequency of the a_2 and b NMR vs the field applied perpendicular to the c axis at 4.2 °K. This is to be compared with the same measurements at 1.4 °K shown in Fig. 3. Note the increased deviation of the b resonance from the $\gamma^{53} H_0$ line at the higher temperatures.

quadrupolar splitting is identical with that which was found for the a resonance nuclei when they were rotated into the c plane.

The penetration of the external field should result in a decrease of the resonance frequency which would vary linearly with $H_0^\perp$ only if the field and spin moments are *parallel*. Hence two facts must be explained: (a) the apparent absence of spins oriented *antiparallel* to H_0, and (b) the initial smaller decrease of the resonance frequency than would be expected for almost complete field penetration. If the perpendicularly oriented spins reside at the center of the walls, the application of a field in the plane will cause them to rotate until they are parallel to the field, since the in-plane anisotropy is so small. Thus only one resonance should appear since the free energy is lowest for the parallel configuration. As to the initial slope of the resonance, we note that the deviation from the expected $\gamma_n H_0(1 - H_d^\perp/H_s^\perp)$ at low fields and 1.4 °K presumably results from the finite spin sus-

ceptibility at this temperature. In Fig. 9 we show that if the temperature is raised to 4.2 °K the increased perpendicular susceptibility further enhances the deviation from the simple $\gamma_n H_0(1 - H_d^\perp/H_s^\perp)$ behavior expected for the resonance. It is our belief that at 0 °K, with zero perpendicular susceptibility, the initial slope of the b resonance would indeed be $\gamma_n H_0(1 - H_d^\perp/H_s^\perp)$. The effect that the *parallel* susceptibility has on the NMR in the saturated state, at elevated temperatures, has been discussed previously. [5]

Hence, from the field dependence and structure of the a and b resonances we can identify the *orientation* of the electronic spins whose nuclei contribute to the resonances—a resonances arise from spins oriented parallel to the c axis and b resonances from spins oriented perpendicular to that axis—but we cannot unambiguously locate the spins in either case. To elucidate the problem we now consider the enhancement and rf polarization measurements.

TABLE II. CrBr$_3$ parameters.

	Value
Transverse exchange J_T	8.25 °K
First anisotropy K	-9.3×10^5 erg/cm^3
Anisotropy field H_A	6.8 kOe
Lattice constant a	3.66 Å
Lattice constant c	18.30 Å
Sample thickness T	~ 0.5 cm
Saturation mag. M_s	0.270 kOe
Curie temperature T_C	32.5 °K
Domain wall thickness δ_W	120 Å
Bulk domain width d	2.4×10^5 Å

D. Enhancements and Relative Signal Intensities

In ferromagnets the primary mechanisms for enhancement of the rf field at the nucleus via the hyperfine interaction arise from either domain rotation or domain wall motion.[16] Because the enhancement due to the latter is expected to be so much larger, a meaningful observation of domain-rotation enhancement can only be had when there are no walls present. In the *saturated* state the domain-rotation enhancement η_D may be expressed as $\eta_D = H_n/H_m$, with H_n the hyperfine field and H_m the field which restricts the rotation of the domain. By minimizing the total energy we find, for *small* rotations of the electronic spins,

$$\eta_D^{\parallel} = H_n^{\perp}(H_0^{\parallel} - H_s^{\parallel} + H_s^{\perp})^{-1}, \quad \vec{H}_{rf} \perp \vec{c} \tag{4a}$$

$$\eta_D^{\perp} = H_n^{\parallel}(H_0^{\perp} - H_s^{\perp} + H_s^{\parallel})^{-1}, \quad \vec{H}_{rf} \parallel \vec{c} \tag{4b}$$

$$\eta_D^{\perp} = H_n^{\perp}(H_0^{\perp})^{-1}, \quad \vec{H}_{rf} \perp \vec{c} \text{ and } \vec{H}_0^{\perp}. \tag{4c}$$

In Fig. 5 we compare the predictions of Eqs. (4a)–(4c) with the experimental results. Only relative measurements of enhancement versus field were made, and these are seen to be in reasonable agreement with the theory for both directions of H_0. The absolute magnitudes of η_D are of some interest, if only to see how small they are relative to η_W, the wall-motion enhancement. For example, we calculate $\eta_D^{\parallel}(H_0 = H_s^{\parallel}) \approx 30$, whereas we expect the maximum enhancement at the center of a wall to be $\eta_W \approx 5 \times 10^5$, as we shall now show.

If we assume the sample magnetizes by wall displacement in, say, the x direction when H is applied parallel to the c axis, then the wall displacement Δx, per unit field, is $\Delta x = d/H_s^{\parallel}$, with d the width of the domain. Assuming $H_{rf} \parallel c$ we have for the wall displacement enhancement

$$\eta_W(x_0) = d\left(\frac{H_n}{H_s^{\parallel}}\right)\left(\frac{d\Phi}{dx}\right)_{x_0}, \tag{5}$$

where $d\Phi/dx$ is the angular rotation rate of the spins in the wall and varies as a function of the distance x_0 from the center of the wall. At the center $(d\Phi/dx)_0 = (A/K)^{-1/2}$, where $A = 2JS^2/a$ and

J and a are the exchange energy per spin and the near-neighbor Cr^{3+}-Cr^{3+} spacing, respectively, and K is the anisotropy energy per unit volume.[17] Using the parameters in Table II we find $\eta_W = 55 \times 10^4$, which is more than 10^4 times as large as η_D !

Since $\eta_W \approx \eta_b$, it is clear that wall enhancement is responsible for the b resonance. More significant is the fact that, since η_a is more than three orders of magnitude larger than any reasonable estimate of η_D, domain rotation *cannot* be responsible for the a resonance, and *hence the nuclei in question cannot reside inside the domain*. But if the a resonance arises from spins which are oriented collinearly with the c axis, and the spins are not inside the domains, then they must be at the edge of the 180° walls and have their signal enhanced by the same motion of the walls that produces the b resonance.

The possibility of wall motion enhancing a "domain-edge" resonance was first suggested by Turov *et al.*[18] using a Green's-function approach to the problem. We wish to explore this idea in the context of the simpler Murray–Marshall[19] formalism. The power spectrum associated with the NMR in a 180° wall is given by

$$P(\nu) = \int_0^\pi q(\Phi)f(\nu - \nu')\,d\Phi , \tag{6}$$

where $q(\Phi)$ is the strength of the signal coming from nuclei in the wall whose quantization direction makes an angle Φ with the easy direction and $f(\nu - \nu')$ is the contribution to the line profile at frequency ν'. From Ref. 19 we know that

$$q(\Phi)\,d\Phi = k\eta_\Phi^2 H_{rf}^2 n(\Phi)\,d\Phi , \tag{7}$$

where $\eta_\Phi = \eta_0 \sin\Phi$ is the enhancement factor as a function of angle, k is a constant, $n(\Phi)\,d\Phi$ is the number of spins pointing between Φ and $\Phi + d\Phi$, and H_{rf} is the applied rf field. Since the number of spins per unit distance is a constant, $n(x) = n_0/d$, then $n(\Phi) = (n_0/d)\,dx/d\Phi$. But $\sin\Phi = \text{sech}(\pi x/\delta_W)$ with $\delta_W = \pi(A/K)^{1/2}$, d the domain thickness, and n_0 the total number of spins in a domain. Therefore, $dx/d\Phi = -\delta_W/\pi \sin\Phi$ and $n(\Phi) = (n_0\delta_W/d\pi)\,|1/\sin\Phi|$, with the absolute value necessary because $n(\Phi)$ is always a positive quantity.

Murray and Marshall assumed the intrinsic linewidth to be independent of position in the wall and hence independent of frequency and Φ. In keeping with the ideas of Turov *et al.* we now assume that the linewidth Δ *does* depend on position relative to the center, i.e., that $\Delta = \Delta(\Phi)$ and, furthermore, that the line profile is Lorentzian. We have

$$f(\nu - \nu') = \frac{\Delta}{\pi}\,\frac{1}{\Delta^2 + (\nu - \nu')^2} , \tag{8}$$

with $\nu' = \nu_d - \delta\nu\sin^2\Phi$ and $\Delta(\Phi) = \Delta_d + \delta f(\Phi)$. Since the composite line shape does not change appreciably with temperature, we believe $\Delta(\Phi)$ to be inde-
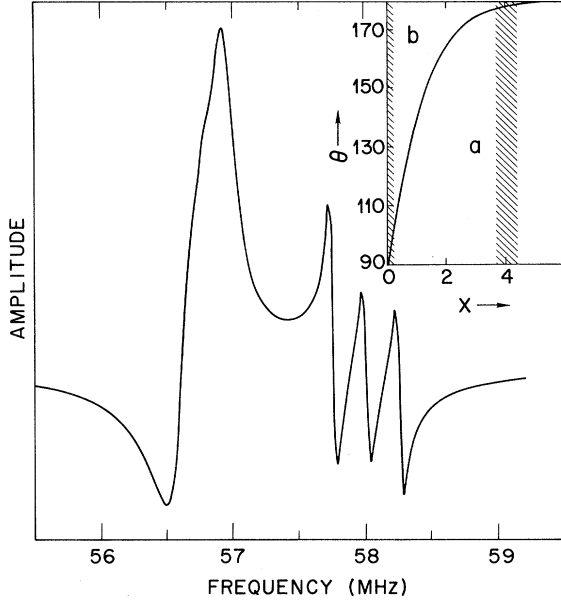
FIG. 10. Predicted spectrum for the wall-enhanced
Cr^{53} NMR using the model discussed in the text. The
amplitude and frequency scale are adjusted so as to make
possible direct comparison with the observed spectrum
shown in Fig. 1. The intrinsic linewidth is assumed to
vary as $\Delta_d + \delta \sin^2\theta$ through the wall. The solid line in
the insert is the angle that the spins make with respect
to the c axis as a function of $X = (A/K)^{1/2}$, the distance
from the wall center. The shaded areas indicate the re-
gions in the wall which mainly contribute to the two reso-
nances. The "classical" wall thickness δ_W is equal to
πX.

pendent of temperature. This contrasts with the
behavior supposed by Turov *et al.*, where the
origins of the Φ-dependent linewidth came from
thermal magnon scattering associated with the
low-energy excitations peculiar to the wall (trans-
lational or breathing modes). We assume that
these same excitations allow for a strong indirect
coupling between nuclei through a Suhl–Nakamura[20]
interaction. Since the amplitude of these excita-
tions is largest at the wall center and vanishes at
the edge of the wall, one expects a position-dependent
linewidth. The exact functional form of this depen-
dence is not clear. From considerations of the ampli-
tude of the wall excitation alone, one would expect
a $\sin^2\Phi$ dependence.[21] However, because of the
anisotropic hyperfine interaction, the number of
nuclei that can interact, and therefore the range
of the interaction, also depends on Φ. For illus-
trative purposes we will assume a $\sin^2\Phi$ depen-
dence. We have then for the power spectrum

$$P(\nu) \propto \int_0^\pi \frac{|\sin\Phi| (\Delta_d + \delta \sin^2\Phi) d\Phi}{(\Delta_d + \delta \sin^2\Phi)^2 + (\nu - \nu_d + \delta\nu \sin^2\Phi)^2} \quad .$$

(9)

Because of the large enhancements of the rf field
in ferromagnets, the absorptive component of the
nuclear susceptibility ($\chi_n^{||}$) usually saturates at
relatively low driving fields. The power absorp-
tion then arises from the modulation of the elec-
tronic losses ($\chi_e^{||}$) by the dispersive part of χ_n,
i.e., χ_n'. This results in the observed power spec-
trum being dependent upon χ_n' as follows:

$$P(\nu) \propto \int_0^\pi \frac{|\sin\Phi| (\nu - \nu_d + \delta\nu \sin^2\Phi) d\Phi}{(\Delta_d + \delta \sin^2\Phi)^2 + (\nu - \nu_d + \delta\nu \sin^2\Phi)^2} \quad .$$

(10)

We have attempted to qualitatively reproduce the
observed resonance profile (Fig. 1) by adjusting
δ and $\delta\nu$, assuming that only the dispersive part
of χ_n is observable and hence that Eq. (10) applies.
A satisfactory reproduction of the general fea-
tures of Fig. 1 may be obtained using the known
values of $\delta\nu$ and ν_d, choosing $\Delta_d = 30$ kHz and δ
$= 120$ kHz and including the appropriate quadrupo-
lar structure. The result is shown in Fig. 10. If
we assume there is no angular dependence to the
linewidth (i.e., $\delta \equiv 0$), we would find the b reso-
nance to exhibit quadrupolar structure, as shown
in Fig. 11.

There are a number of interesting features to
the calculation and its comparison with experi-
ment: (i) The observed b and a resonances are
seen to arise from nuclei at the center and edge
of the walls, respectively. (ii) The apparent
width of the b resonance requires that $\Delta = \delta + \Delta_d$
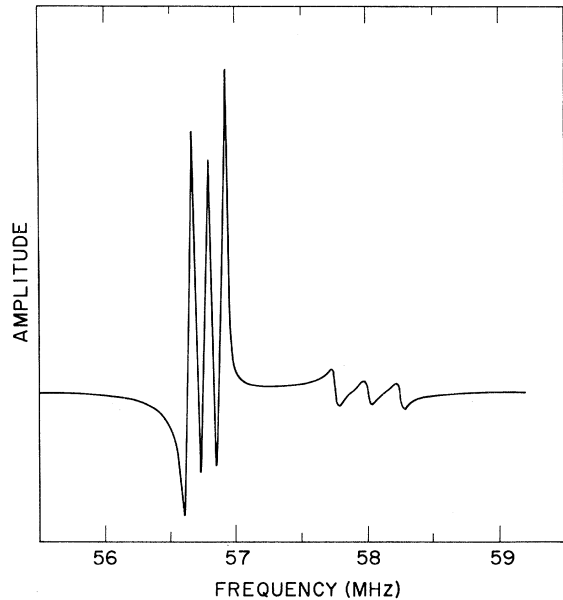near the center of the wall be much larger than one

FIG. 11. Predicted spectrum for the wall-enhanced
Cr^{53} NMR using the same model as was used for Fig. 10,
except that the intrinsic linewidth is assumed to be con-
stant ($\Delta = \Delta_d$) through the wall.

would expect from inhomogeneous broadening and not equally affect the spins at the edge of the wall. For example, if we suppose that the spins at the center deviate by as much as $5°$ from the perpendicular to the c axis (this is the angular separation between the center and nearest-neighbor spins in the wall) there would result only an rms width of less than 20 kHz. Hence inhomogeneous broadening does not account for the width, which then must have a dynamic origin. This is in keeping with our failure to see either a free-induction-decay or spin-echo signal, since $\delta^{-1} \lesssim 1$ μsec, which is much less than the amplifier recovery time used to observe the transient signal. (iii) The absence of quadrupolar structure at the b resonance position implies that δ must be comparable with the separation between quadrupolar components. (iv) The rather large value of T_2^q is consistent with the assumed position dependence of δ and the diminished wall excitations at the wall edge. (v) The largest contribution to the a resonance comes from spins which deviate by about $2°-3°$ from being aligned along the c axis whose enhancement is $\simeq 0.05\eta_0$, where η_0 is the enhancement at the wall center. This ratio is in good agreement with the values given in Table I.

E. rf Polarization and Rotary Saturation Results

The model assumed to explain the line shape has implicit in it that any small element of the wall moves uniformly in response to the driving rf field. It does not follow that, in the real crystal, all walls are displaced by the same amount under the influence of a given field or that the displacement will have the polarization dependence expected for c-oriented domains separated by $180°$ walls. As such, both the observed rf polarization results and the a resonance rotary-saturation behavior are considerably more difficult to interpret than they would otherwise be.

Concerning the dependence of the enhancement on orientation of the rf field as shown in Table I, we note that in the model assumed above wall displacement enhancement should obey a $\cos\theta$ relation, where θ is the angle between the c axis and H_{rf}. Two properties of the real crystal militate against this simple behavior: (a) The domain structure of CrBr₃ is known to be labyrinthlike, rather than of the ideal slab form, as a result of the small in-plane anisotropy; (b) the directions taken by the spins at the centers of the walls have a considerable spread in the basal plane. The former property most likely results in some displacement of walls in particular regions of the sample under the influence of a driving field applied in the basal plane. The latter property could result in a distribution of enhancements from the following mechanism. If one had parallel slabs

(say, in the y-z plane) and $\vec{H}_{rf} \parallel \vec{y}$, then some of the "wrong"-pointing spins at the center of walls would want to rotate towards the instantaneous direction of H_{rf} to minimize their magnetic energy. This would apply to roughly half the spins in the walls, since half of the center spins are along the $+y$ and half along the $-y$ directions initially so as to minimize the wall demagnetizing energy. If we assume that the spins rotate smoothly and that the wall demagnetizing energy limits their motion, we find a maximum enhancement $\eta \approx \pi(H_{hf}/H_d^{\perp})(d/\delta_W)$, which, in fact, is $H_d^{\parallel}/H_d^{\perp}$ larger than what is obtained for $\vec{H}_{rf} \parallel \vec{c}$. This wall-rotation enhancement would take place even in the ideal-slab model discussed above. However, the labyrinthlike structure ensures that H_{rf} will have varying projections on a given wall plane so we would expect to find a distribution of values of η.

Likewise, the rotary-saturation measurements of the enhancement will reflect the distribution of wall displacements for a given strength of H_{rf}, either because of the labyrinthlike nature of the domain structure or as a result of wall-pinning effects, as has been discussed by Stearns.[22] In addition, we would expect the a resonance to exhibit a variation in enhancements since this is intrinsic to its origin. However, we caution that it would be misleading to interpret the rotary-saturation signal as presented as a weighted measure of the number of spins that have an intrinsic enhancement times the enhancement because of the effects discussed above.

V. CONCLUSIONS

From the magnitude and orientation dependence of the Cr⁵³ NMR spectrum in CrBr₃ we have shown that both a and b resonances arise from wall motion. The a and b resonances are associated with spins at the edge and at the center of the walls, respectively. However, to reproduce the general features of the line profile it is essential to include a position-dependent linewidth within the wall, as was first proposed by Turov et al.[18] We have shown how the essential properties of the Turov et al. model may be more simply obtained from an extension of the Murray–Marshall[19] model. We believe that the results obtained by Nagai et al.[23] on MnP also reflect the importance of a position-dependent linewidth associated with wall-enhanced center and edge resonances.

It was believed initially[2,3] that the a and b resonances in CrBr₃ were domain rotation enhanced and wall displacement enhanced, respectively. Later[24] it was thought that the b resonance arose from the motion of spins in domains of closure. Not only are closure domains energetically unfavorable because of the large values of K/J, but our analysis shows there is no need to invoke them if proper

consideration is given to the orientation dependence of the field on the resonance frequency at the center of the wall and the position dependence of the linewidth in the wall.

One important conclusion to be drawn from our work is that in a ferromagnetic crystal, where the calculated values of η_W/η_D are large, it is unlikely that a domain-rotation-enhancement NMR will be

seen in the unsaturated state. This is true irrespective of whether an anisotropic hyperfine interaction exists or not.

ACKNOWLEDGMENTS

*Research at UCSB supported in part by the National Science Foundation.

†Work performed in part while at the University of California, Santa Barbara, Calif.

[1]I. Tsubokawa, J. Phys. Soc. Japan 15, 1664 (1960).

[2]A. C. Gossard, V. Jaccarino, and J. P. Remeika, Phys. Rev. Letters 7, 122 (1961).

[3]A. C. Gossard, V. Jaccarino, and J. R. Remeika, J. Appl. Phys. 33, 1187S (1962).

[4]H. L. Davis and A. Narath, Phys. Rev. 134, 433 (1964).

[5]C. H. Cobb, V. Jaccarino, J. P. Remeika, R. Silberglitt, and H. Yasuoka, Phys. Rev. B 3, 1677 (1971).

[6]J. F. Dillion, Jr. and M. Teague, Rev. Sci. Instr. 35, 747 (1964).

[7]R. G. Shulman, Phys. Rev. 121, 125 (1961).

[8]An Arenberg Ultrasonic Laboratory PG-650C pulsed oscillator modulated by a General Radio 1395A modular pulse generator formed the incoherent pulses.

[9]A. G. Redfield, Phys. Rev. 98, 1787 (1955).

[10]E. F. Mendis and L. W. Anderson, Phys. Rev. B 2, 569 (1970).

[11]H. Abe, H. Yasuoka, and A. Hirai, J. Phys. Soc. Japan 21, 77 (1966).

[12]I. Solomon, Phys. Rev. 110, 61 (1958).

[13]D. L. Cowan and L. W. Anderson, Phys. Rev. 135, A1046 (1964).

[14]J. F. Dillion, Jr. and J. P. Remeika, J. Appl. Phys. 34, 637 (1963).

[15]A. Abragam, Principles of Nuclear Magnetism (Oxford U. P., London, 1961), p. 234.

[16]A. M. Portis and A. C. Gossard, J. Appl. Phys. 31, 2055 (1960).

[17]S. Chikazumi, Physics of Magnetism (Wiley, New York, 1964), p. 186.

[18]Y. A. Turov, A. P. Tankeyev, and M. I. Kurkin, Fiz. Metal. i Metalloved. 28, 385 (1969); 29, 747 (1970).

[19]G. A. Murray and W. Marshall, Proc. Phys. Soc. (London) 86, 315 (1965).

[20]H. Suhl, Phys. Rev. 109, 606 (1958); T. Nakamura, Progr. Theoret. Phys. (Kyoto) 20, 542 (1958).

[21]J. M. Winter, Phys. Rev. 124, 452 (1961).

[22]M. B. Stearns, Phys. Rev. 162, 496 (1967).

[23]H. Nagai, T. Hihara, and E. Hirahara, J. Phys. Soc. Japan 29, 622 (1970).

[24]C. H. Cobb and V. Jaccarino, J. Appl. Phys. 42, 1310 (1971).

Spin Polarization of Electrons Tunneling from Films of Fe, Co, Ni, and Gd†

P. M. Tedrow and R. Meservey

Francis Bitter National Magnet Laboratory, Massachusetts Institute of Technology, Cambridge, Massachusetts 02139

(Received 1 February 1972; revised manuscript received 2 August 1972)

The spin polarization of electrons tunneling from films of Fe, Co, Ni, and Gd to superconducting Al films is determined from conductance measurements. The phenomenological theory of superconducting–normal-metal tunneling is modified to describe superconducting-ferromagnetic tunneling in a magnetic field. The experimental technique and the method of analysis of the conductance curves to obtain the electron polarization are both described. The observed polarization is positive (majority spin direction predominating) for all the metals; the values obtained were Fe, +44%; Co, +34%; Ni, +11%; and Gd, +4.3%.

I. INTRODUCTION

Spin polarization of electrons emerging from ferromagnetic materials has recently been the subject of several investigations. Busch and co-workers[1] have measured the spin polarization of photoelectrons emitted from various ferromagnetic films including Fe, Ni, Co, and Gd. Tedrow and

Meservey[2] measured the spin-dependent tunneling between thin films of superconducting Al and ferromagnetic Ni. Gleich and co-workers[3] have studied the spin polarization of field-emitted electrons from different lattice directions of single crystal Ni.

The technique of producing spin-polarized tunneling currents was discovered by Meservey, Ted-